# Spin-orbit-split subbands in IV-VI asymmetric quantum wells

M. M. Hasegawa and E. A. de Andrada e Silva
*Instituto Tecnológico de Aeronáutica, CTA, São José dos Campos, SP, Brazil*
*and Instituto Nacional de Pesquisas Espaciais C.P. 515, 12201 São José dos Campos, SP, Brazil*
(Received 9 April 2003; published 18 November 2003)

Analytical solutions for the spin-orbit-split electron and hole subband structure in IV-VI lead-salt semiconductor asymmetric quantum wells (QW's) are obtained within the envelope function approximation and the Dimmock four-band $k\cdot p$ model for the bulk, around the four equivalent $L$ points. Contrary to the III-V and II-VI QW's, the spin-orbit interaction in the these rocksalt QW's is purely Rashba, although multivalley and anisotropic. The Rashba splitting in these QW's is shown to be highly dependent on the structure parameters and can be much larger than those in similar III-V structures. In particular, specific results for the energy spectrum of $Pb_{1-x}Eu_xTe/PbTe/Pb_{1-y}Eu_yTe$ QW's show that the Rashba splitting is approximately linear (and changes sign) with $\delta Q$, the difference between the band offsets at the two interfaces, independently of the valley and growth direction. The well width and $k_\parallel$ dependences of the Rashba splitting are also investigated, for the ground and excited states confined in IV-VI QW's, and experimental verification of the main predictions is discussed.

DOI: 10.1103/PhysRevB.68.205309 PACS number(s): 73.21.Fg

## I. INTRODUCTION

The spin-orbit coupling, in particular the Rashba term, for electrons in semiconductor nanostructures form the basis of different proposals for new spintronic devices[1,2] and has been attracting much attention. Together with the techniques of semiconductor band-gap (or orbital) engineering, the spin-orbit interaction permits spin manipulation within nonmagnetic structures. In particular, promising spin filtering effects in multibarrier asymmetric III-V nonmagnetic structures have been demonstrated theoretically.[3,4] The in-plane conducting states in these structures are not spin degenerate and the energy splitting between the states with the same $\vec{k}_\parallel$ and opposite spins can be described by an effective ($k_\parallel$-dependent) magnetic field, which determines the spin-dependent properties of the structure. Experimental realization of the mentioned devices has, however, shown to be not easy. Further investigation of the Rashba effect in new structures with new materials should help the understanding of the physics involved and the development of actual devices.

Here, *a theoretical study* is presented of the spin-orbit-split subbands in IV-VI lead-salt (PbTe, PbS, and PbSe) asymmetric QW's, which demonstrates the existence in these structures of a strong Rashba effect, which, besides being a first example of a multivalley and anisotropic Rashba effect, is also highly dependent on the main structure parameters.

It is worth recalling that the spin-orbit splitting in GaAs and narrower-gap III-V QW's has been observed and measured by many different groups[5] and the results have been shown to be in reasonably good agreement with multiband envelope function calculations.[6] More recently, there have been also reports of large spin-orbit splittings observed in GaN (Ref. 7) and HgTe (Ref. 8) QW's. The splitting in IV-VI asymmetric QW's is also expected to be large, due to the strong spin-orbit interaction in these compounds. More important yet is that, since the lead-salt bulk presents inversion symmetry, their QW's present the advantage of a spin-orbit splitting which is purely Rashba.[9] With the recent appearance of both new experimental techniques to study the Rashba effect[10] and high-quality IV-VI thin QW's, our results shall contribute to a better understanding of this important spin-dependent property of the semiconductor nanostructures.

Symmetric molecular-beam-epitaxy (MBE) lead-salt semiconductor QW's have been fabricated and studied by different groups.[11] Transitions between quantized electron- and hole-confined states as well as the break of valley degeneracy have been clearly observed[12] and well described by the envelope function theory.[13] Such theory is here extended to asymmetric QW's and to the study of the break of spin degeneracy due to the Rashba effect. Within the Dimmock $k\cdot p$ model for the bulk, we obtain analytical expressions for the spin-orbit coupling parameter and for the effective magnetic field, in each nonequivalent valley and for QW's grown along different directions.

Next, we describe the model and solution for the energy spectrum of asymmetric IV-VI QW's. Specific results for $Pb_{1-x}Eu_xTe/PbTe/Pb_{1-y}Eu_yTe$ are then presented and finally, in the conclusions, we summarize the main predictions and discuss possible experimental setups for verification.

## II. TWO-BAND MODEL FOR THE RASHBA EFFECT IN IV-VI QW'S

The Rashba effect in asymmetric IV-VI quantum wells can be easily described with the following Kane-like two-band (four including spin) $k\cdot p$ Hamiltonian,[14] which models accurately the bulk band structure in the fundamental gap region around each of the four equivalent $L$ points of the Brillouin zone:

 

$$H=\begin{pmatrix} h_c & h_{cv} \\ h_{vc} & h_v \end{pmatrix}=\begin{pmatrix} \frac{E_g}{2} & 0 & P_l k_z & P_t(k_x-ik_y) \\ 0 & \frac{E_g}{2} & P_t(k_x+ik_y) & -P_l k_z \\ P_l k_z & P_t(k_x-ik_y) & -\frac{E_g}{2} & 0 \\ P_t(k_x+ik_y) & -P_l k_z & 0 & -\frac{E_g}{2} \end{pmatrix}, \tag{1}$$

where $E_g$ stands for the band gap, $P_l$ and $P_t$ are the longitudinal (along [111]) and transverse momentum interband matrix elements, $\vec{k}=(k_x,k_y,k_y)$ is the electron wave vector measured from the $L$ point, and a Cartesian system of coordinates with the $z$ axis along [111] is being used. The upper and lower blocks correspond to the spin-degenerate $L_6^-$ conduction and $L_6^+$ valence bands, respectively.

In the QW case, the same model Hamiltonian is used throughout the structure. The allowed electronic energy levels are obtained from the solution of the eigenvalue problem of the effective Hamiltonian, obtained from the bulk Hamiltonian, Eq. (1), by letting the band gap vary along the growth direction, substituting $\vec{k}$ by $-i(d/dx,d/dy,d/dz)$ and adding the discontinuity of the center-of-gap position $G$ to the diagonal elements, describing the band offset.

In order to better identify the Rashba term, it is useful to reduce the corresponding set of four coupled first-order differential equations into a set of two coupled second-order differential equations, which can be written as

$$H_e F_c=[h_c+h_{vc}(E-h_v)^{-1}h_{cv}]F_c=EF_c, \tag{2}$$

where $F_c=(f_+,f_-)$ is the conduction-band envelope function spinor with a component for each spin orientation and $E$ is the electron energy. Note that $H_e$ depends on the growth direction, which can be oriented differently with respect to different valleys, and in this case they are no longer equivalent.

We will consider explicitly the cases of the two preferential directions for the growth of these structures: [111] and [100]. In the case of [111] QW's, we have one valley along the growth direction (longitudinal valley) and the other three along directions making an angle $\theta=\cos^{-1}(\frac{1}{3})$ with the growth direction (oblique valleys). In [100] QW's they are all oblique with $\theta=\cos^{-1}(1/\sqrt{3})$. The projection of these different valleys in the plane perpendicular to the growth direction is illustrated in Fig. 1 for both [111] and [100] QW's. Neglecting intervalley mixing, we treat each kind of valley separately.

For the longitudinal valley, we have the growth direction along $z$ (the valley main axis), so that $E_g$ depends only on $z$, and $(k_x,k_y)$ are good quantum numbers. We then set $\vec{k}=(k_x,k_y,-id/dz)$, substitute in Eq. (2), and obtain the following Schrödinger-like equation with explicit Rashba spin-orbit coupling:

$$\left[\left(-\frac{\hbar^2}{2}\frac{d}{dz}\frac{1}{m_1}\frac{d}{dz}+\frac{\hbar^2k_x^2}{2m_2}+\frac{\hbar^2k_y^2}{2m_3}+\frac{E_g(z)}{2}+G(z)\right)I_{2\times 2}+\alpha_{so}\vec{B}_{eff}(\vec{k}_\parallel)\cdot\vec{\sigma}\right]F_c=EF_c, \tag{3}$$

where we have defined

$$\vec{B}_{eff}(\vec{k}_\parallel)=\vec{k}_\parallel\times\hat{z} \tag{4}$$

and the spin-orbit coupling parameter

$$\alpha_{so}=\alpha_{so}(z,E)=\frac{d}{dz}\beta_{so}=P_lP_t\frac{d}{dz}\left(\frac{1}{E+\frac{E_g(z)}{2}-G(z)}\right), \tag{5}$$

$\vec{\sigma}$ is the vector of the Pauli spin matrices and the effective masses are $m_1=m_l$ and $m_2=m_3=m_t$, with

$$m_{l,t}=m_{l,t}(z,E)=\frac{\hbar^2}{2P_{l,t}^2}\left(E+\frac{E_g(z)}{2}-G(z)\right). \tag{6}$$

Note that in IV-VI QW's, for the longitudinal valley, we have an isotropic Rahsba spin-orbit coupling, like in III-V QW's, but with a different coupling parameter.

Some more algebra is needed for the oblique valleys. In this case, the Hamiltonian in Eq. (1) is written using a system of coordinates $(x',y',z')$ (see Fig. 2) with none of the axis along the growth direction. It is then convenient to use the

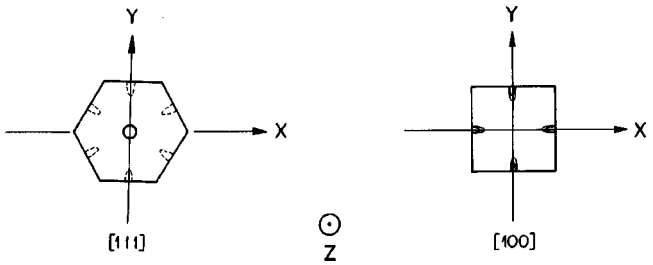


FIG. 1. Projection of the four lead-salt valleys in the plane perpendicular to the growth direction for both [111] and [100] QW's. For [111] samples we have $x$ parallel to [110] and $y$ to [112] crystallographic directions, while for growth along [100], they are instead parallel to [011] and [011], respectively.

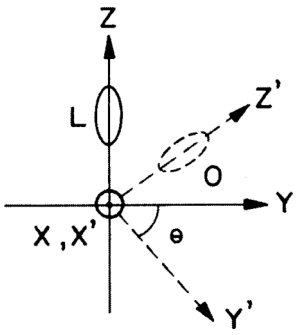


FIG. 2. Illustration of the two sets of coordinate axes for nonequivalent valleys.

rotated system $(x,y,z)$, with $z$ along the growth direction. By doing so, we arrive at the same Eq. (3) above, for the allowed states from the oblique valleys, except for the redefined effective masses and effective field; now we have $m_1 = m_l m_t/(m_t\cos^2\theta + m_l\sin^2\theta)$, $m_2 = m_t$, $m_3 = m_t\cos^2\theta + m_l\sin^2\theta$, and

$$\vec{B}_{eff}(\vec{k}_\parallel) = (-k_y, k_x(r\sin^2\theta + \cos^2\theta), k_x(r-1)\cos\theta\sin\theta), \tag{7}$$

where $r = P_t/P_l$ gives the degree of valley anisotropy. In Table I we summarize the results for the effective field in structures grown along the two main growth directions. One should note that for the oblique valleys the effective field depends on the degree of valley anisotropy $r$ and reduces to the longitudinal case in the spherical $r=1$ limit; we also see that in general though, opposed to the III-V or longitudinal Rahsba effect, their spin-orbit splitting is described by an effective field with nonzero component along the growth direction and an absolute value which is not isotropic in the $k_\parallel$ plane.

### III. $Pb_{1-x}Eu_xTe/PbTe/Pb_{1-y}Eu_yTe$ ASYMMETRIC QW'S

Good-quality PbEuTe/PbTe QW's have been grown by different groups and, as a simple and practical example, we consider here the solution of Eq. (3) to calculate the allowed energy levels of [111] $Pb_{1-x}Eu_xTe/PbTe/Pb_{1-y}Eu_yTe$ QW's. Neglecting any band bending in view of the large static dielectric constant of these materials, we have plane-wave solutions in each piece of bulk, with wave vectors

$$q = \pm\sqrt{\frac{2m_{1,w}}{\hbar^2}\left(\varepsilon - \frac{E_g^w}{2}\right) - \frac{m_{1,w}}{m_{2,w}}k_x - \frac{m_{1,w}}{m_{3,w}}k_y} \tag{8}$$

in the well and

$$\chi_i = \pm\sqrt{\frac{2m_{1,b_i}}{\hbar^2}\left(\frac{E_g^{b_i}}{2} + G_i - \varepsilon\right) + \frac{m_{1,b_i}}{m_{2,b_i}}k_x + \frac{m_{1,b_i}}{m_{3,b_i}}k_y}, \quad i = r,l, \tag{9}$$

TABLE I. Effective magnetic field for the Rahsba effect in lead-salt quantum wells grown along [111] and [100].

| | $B_z$ | $B_x$ | $B_y$ | $\lvert B_{eff}\rvert(r=\sqrt{10})$ | Valley $(n_v)$ |
|---|---|---|---|---|---|
| [111] | 0 | $-k_y$ | $k_x$ | $\sqrt{k_x^2+k_y^2}$ | $l(1)$ |
| | $\frac{2\sqrt{2}}{9}(r-1)k_x$ | $-k_y$ | $\frac{8r+1}{9}k_x$ | $\sqrt{9k_x^2+k_y^2}$ | $o(3)$ |
| [100] | $\frac{\sqrt{2}}{3}(r-1)k_x$ | $-k_y$ | $\frac{2r+1}{3}k_x$ | $\sqrt{7k_x^2+k_y^2}$ | $o(4)$ |

in the barriers, where $r$ and $l$ stand for the right and left barriers, respectively. Following Ref. 15, by matching the solutions at the interface, using the spin-dependent boundary condition, i.e.,

$$-\frac{\hbar^2}{2}\frac{1}{m_1}\frac{d}{dz}f_\pm(z) \pm \beta_{so}|\vec{B}_{eff}|f_\pm(z) \quad \text{continuous across the interface,} \tag{10}$$

the allowed energies, as a function of $\vec{k}_\parallel$, are obtained from

$$\left(\frac{\hbar^2 k}{2m_{1,w}}\right)^2 - \frac{\hbar^2 k}{2m_{1,w}tg(qL)}\left[\frac{\hbar^2}{2}\left(\frac{\chi_l}{m_{1,b_l}} + \frac{\chi_r}{m_{1,b_r}}\right) \pm (\beta_{so}^{b_l} - \beta_{so}^{b_r})|\vec{B}_{eff}|\right]$$
$$= \left(\frac{\hbar^2\chi_l}{2m_{1,b_l}} \pm (\beta_{so}^{b_l} - \beta_{so}^{w})|\vec{B}_{eff}|\right) \times \left(\frac{\hbar^2\chi_r}{2m_{1,b_r}} \mp (\beta_{so}^{b_r} - \beta_{so}^{w})|\vec{B}_{eff}|\right), \tag{11}$$

where the $\pm$ sign stands for the spin up or down in the direction of the effective field and $L$ is the well width. Note that $\beta_{so}$, defined in Eq. (5), as well as $m_i$, depend on both material and energy.

The band offset $Q$, defined by $\Delta E_c = Q\Delta E_g$, gives the percentage of the difference in the band gap that goes to the conduction band and is connected to $G$ by $G = (Q - 0.5)\Delta E_g$. It will be used below in the discussion of the results.

Figure 3 gives in the upper part the quantized subbands obtained for electrons confined in the PbTe well, while in the lower the corresponding spin splitting, for $k_\parallel$ along $x$ (i.e., the direction perpendicular to [211], [121], or [112], depending on the specific oblique valley, which are the directions of the projections of the oblique valleys main axis in the plane perpendicular to the growth direction). The states for increasing energy, derived from the longitudinal and oblique valleys, are denoted $(0^L,1^L,2^L,\ldots)$ and $(0^O,1^O,2^O,\ldots)$, respectively, and we recall that the spins correspond always to the quantization axis along the effective field. Bound to this narrow PbTe well, we have only two longitudinal subbands and one oblique (from each of the three equivalent valleys). Note that in every subband the splitting grows initially lin-

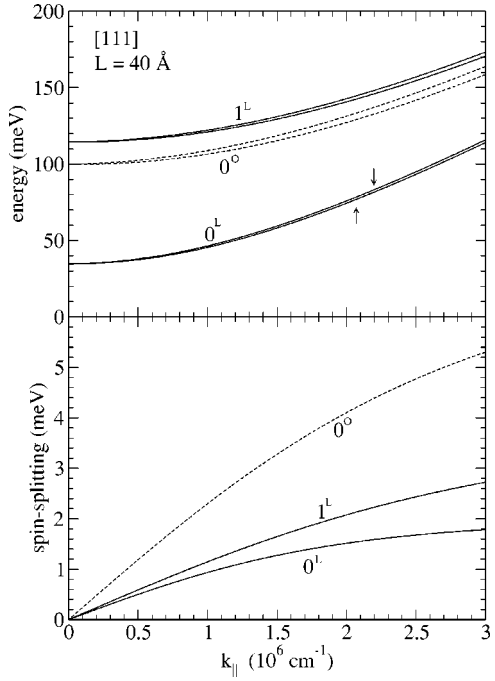


FIG. 3. Electron subbands of a 4-nm [111] $Pb_{0.91}Eu_{0.09}Te/PbTe/Pb_{0.93}Eu_{0.07}Te$ asymmetric quantum well. The subbands, two longitudinal ($0^L$ and $1^L$) and one oblique ($0^O$), are spin split due to the Rashba effect. In the lower panel, the splitting is shown as a function of $k_\parallel$ (along $x$). The band offset used is as illustrated in the inset of Fig. 4—i.e., $Q_1=0.6$ and $Q_2=0.5$—and parameters for $T=5$ K have been used.

early with $k_\parallel$ and then tends to saturate. The splitting in the oblique subband along this direction is 3 times bigger than the corresponding longitudinal.

An important thing to note though is that the results in Fig. 3 correspond to a specific band alignment—i.e., $Q_1=0.6$ and $Q_2=0.5$—as illustrated in the inset of Fig. 4. However, as opposed to the transition energies used to estimate the band offset in these structures, the Rashba splitting is seen to be highly sensitive to the band alignment. This is shown in Fig. 4, where the splitting for a fixed parallel wave

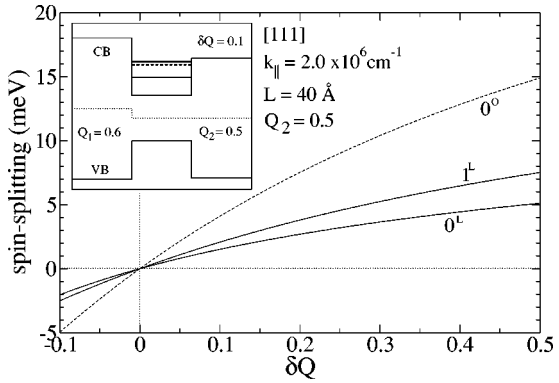


FIG. 4. Rashba spin splitting for a fixed $k_\parallel$ ($2.0\times10^6$ cm$^{-1}$) as a function of $\delta Q=Q_1-Q_2$, the difference between the band offset at the two interfaces, as illustrated in the inset. The structure and parameters are as in Fig. 3.

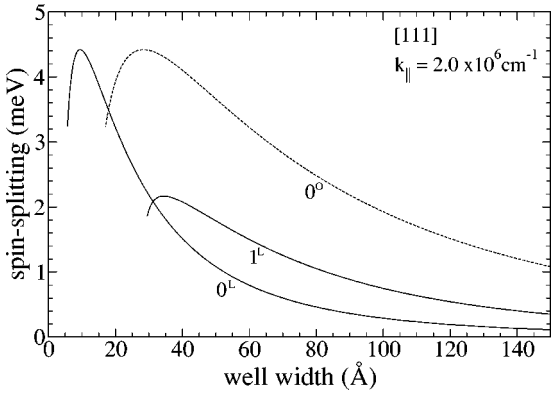


FIG. 5. Well width dependence. The spin splitting, at the different subbands and for a fixed $k_\parallel$, is plotted as a function of the PbTe well width; again the structure and parameters are as in Fig. 3.

vector is shown as a function of $Q_1$, from 0.4 to 1.0 (i.e, for $\delta Q=Q_1-Q_2$, from $-0.1$ to 5.0). The splitting turns out to follow $\delta Q$ almost linearly, so that, besides changing by more than one order of magnitude, the splitting can change sign and be zero depending on the difference between the band offsets at the two interfaces. The zero, or very small, splitting (since the real materials have bands only approximately symmetric) predicted here for asymmetric QW's with the same band offset in both interfaces is a consequence of the perfect specular symmetry between the conduction and valence bands in the two-band model. The origin of the spin-orbit splitting in IV-VI QW's can then be traced down to a more specific mesoscopic asymmetry. It is not enough to have different barrier materials; the band offsets must also be different in order to break the spin degeneracy of the conduction and valence subbands of lead-salt QW's.

Note that, in these PbTe QW's, large splittings, more than one order of magnitude bigger than in similar GaAs QW's, can be obtained. It is due to the stronger spin-orbit coupling for the conducting electrons in IV-VI materials, as indicated also by the following ratio estimated at energies in the middle of the respective barriers:

$$\frac{\beta_{so}^{PbTe}-\beta_{so}^{PbEuTe}}{\beta_{so}^{GaAs}-\beta_{so}^{GaAlAs}}\sim -70. \tag{12}$$

To complete the picture of the Rashba splitting in these PbTe QW's, in Figs. 5 and 6 we show the well width dependence and the anisotropy in the interface or $k_\parallel$ plane, respectively. As in similar III-V QW's, we see the splitting increasing with decreasing well width, reaching a maximum near the critical width for another bound state. Differently from the III-V case, however, we have the two series of subbands, longitudinal and oblique, and in the last ones the splitting is anisotropic. Figure 6 shows the splitting for three different values of the absolute value of $k_\parallel$ as a function of the wave vector direction for the lowest subband of a oblique valley. The splitting is given by the distance from the center to the curves (using the scale in the left). One see that the splitting is much larger for electrons traveling along $x$ (the angles in

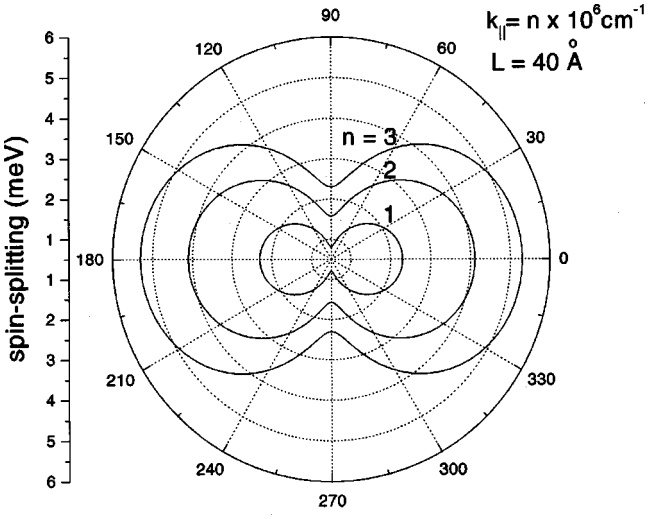


FIG. 6. Rashba splitting anisotropy in the oblique subbands. The spin splitting of the ground oblique subband is plotted as a function of the $k_{\|}$ direction in the plane for different fixed absolute values. For each direction, the splitting is given by the distance from the center to the curve, measured in accordance with the scale on the left. The specific directions are given by the angle with respect to $x$.

Fig. 6 are defined with respect to $x$ direction) than for those traveling along directions perpendicular to it.

## IV. CONCLUSIONS

To conclude, we believe to have given here enough ground for the existence of a Rashba splitting in the conduction and valence subbands of IV-VI asymmetric QW's with unique properties. It is a first example of multivalley and anisotropic Rashba effect. Analytical expressions for both the coupling parameter and effective field were obtained within the envelope function approximation with a two-band (four with spins) $k \cdot p$ model for the bulk. The spin-orbit-split subband structure of PbEuTe/PbTe asymmetric QW's was calculated and studied in detail.

In particular, it is obtained a splitting in all the subbands that is highly sensitive to the asymmetry in the band offset. The band offset in these structures is not well known; the optical transition energies, used to estimate it, are not very band offset sensitive. The possibility to measure the spin splitting in different IV-VI QW structures would then represent a more accurate way to determine the band offset. The increasing concentration of Eu, for instance, seems to affect mainly the valence band, so that we can expect different band offsets at barriers with different concentration of Eu, which could be studied by looking at the spin splitting of the subbands of states confined in PbTe QW's.

Finally, to be compared with specific experiments though, the present semiempirical calculation should be done with parameters (effective masses and band gaps), accounting not just for the right sample temperature and strain, but also corresponding to the specific band (conduction or valence) one is interested. The study of the Rashba effect for the development of spintronic devices may gain simple expressions and clear predictions with this example of semiconductor nanostructure with pure Rashba spin-orbit coupling.

## ACKNOWLEDGMENTS

This research has been supported by FAPESP and CNPq, Brasil. We thank also discussions with Professor G. C. La Rocca and Professor J. R. Senna.

[1] See, for example, M. Johnson, Science **260**, 320 (1993); G. Prinz, Phys. Today **48** (4), 58 (1995); *Spin Electronics*, edited by M. Ziese and M. J. Thornton (Springer, Berlin, 2001); Michael L. Roukes, Nature (London) **411**, 747 (2001).

[2] S. Datta and B. Das, Appl. Phys. Lett. **56**, 665 (1990).

[3] T. Koga, J. Nitta, H. Takayanagi, and S. Datta, Phys. Rev. Lett. **88**, 126601 (2002).

[4] E.A. de Andrada e Silva and G.C. La Rocca, Phys. Rev. B **59**, R15 583 (1999).

[5] See, for instance, B. Das *et al.*, Phys. Rev. B **39**, 1411 (1989); J. Luo, H. Munekata, F.F. Fang, and P.J. Stiles, *ibid.* **41**, 7685 (1990); B. Jusserand, D. Richards, G. Allan, C. Priester, and B. Etienne, *ibid.* **51**, R4707 (1995); C.-M. Hu, J. Nitta, T. Akazaki, H. Takayanagi, J. Osaka, P. Pfeffer, and W. Zawadzki, *ibid.* **60**, 7736 (1999); T. Matsuyama, R. Krsten, C. Meiner, and U. Merkt, *ibid.* **61**, 15 588 (2000); D. Grundler, Phys. Rev. Lett. **84**, 6074 (2000).

[6] See, for instance, G. Lommer, F. Malcher, and U. Rossler, Phys. Rev. Lett. **60**, 728 (1988); E.A. de Andrada e Silva, Phys. Rev. B **46**, 1921 (1992); E.A. de Andrada e Silva, G.C. La Rocca, and F. Bassani, *ibid.* **50**, 8523 (1994).

[7] Ikai Lo, J.K. Tsai, W.J. Yao, P.C. Ho, Li-Wei Tu, T.C. Chang, S. Elhamri, W.C. Mitchel, K.Y. Hsieh, J.H. Huang, H.L. Huang, and Wen-Chung Tsai, Phys. Rev. B **65**, 161306(R) (2002).

[8] X.C. Zhang, A. Pfeuffer-Jeschke, K. Ortner, V. Hock, H. Buhmann, C.R. Becker, and G. Landwher, Phys. Rev. B **63**, 245305 (2001).

[9] The spin-orbit splitting in III-V asymmetric QW's, for instance, has two contributions: one due to the lack of inversion symmetry in the bulk, which for electrons leads to the so-called $k^3$ term, and one due to the lack of specular symmetry in the structure, which corresponds to the Rashba term, the dominant one in structures with narrow-gap compounds, and the one that can be better controlled with the gate voltage. In general though both contributions are present. It has been shown, for example, that when they are comparable, their interplay leads to a sizable anisotropy in the splitting, which is then dependent on both growth and $\vec{k}_{\|}$ directions. However, it has not been easy to distinguish the two contributions. With the IV-VI asymmetric QW's one can better study the Rashba effect.

[10] See, for instance, K. Yoh *et al.* (unpublished); T. Kikutani *et al.* (unpublished).

[11] A. Ishida, S. Matsuura, M. Mizuno, and H. Fujiyasu, Appl. Phys. Lett. **51**, 478 (1987); S. Yuan, G. Springholz, G. Bauer, and M.

Kriechbaum, Phys. Rev. B **49**, 5476 (1994); I.I. Zasavitskii, E.V. Bushuev, S.O. Ferreira, P. Motisuke, and I.N. Bandeira, Superlattices Microstruct. **24**, (1998); H.Z. Wu, N. Dai, M.B. Johnson, P.J. McCann, and Z.S. Shi, Appl. Phys. Lett. **78**, 2199 (2001); I.I. Zasavitskii, E.V. Bushuev, E.A. de Andrada e Silva, and E. Abramof, JETP Lett. **75**, 559 (2002); H. Wu, N. Dai, and P.J. McCann, Phys. Rev. B **66**, 045303 (2002).

[12] E. Abramof, E.A. de Andrada e Silva, S.O. Ferreira, P. Motisuke, P.H.O. Rappl, and A.Y. Ueta, Phys. Rev. B **63**, 085304 (2001).

[13] E.A. de Andrada e Silva, Phys. Rev. B **60**, 8859 (1999).

[14] See, for instance, J.O. Dimmock, in *The Physics of Semimetals and Narrow Gap Semiconductors*, edited by D.L. Carter and R.T. Bate (Pergamon, New York, 1971), p. 319.

[15] E.A. de Andrada e Silva, G.C. La Rocca, and F. Bassani, Phys. Rev. B **55**, 16 293 (1997).